MOLECULAR AND CELLULAR BIOLOGY, Mar. 2003, p. 1602–1613 Vol. 23, No. 5
0270-7306/03/$08.00+0 DOI: 10.1128/MCB.23.5.1602–1613.2003

Delayed rRNA Processing Results in Significant Ribosome Biogenesis and Functional Defects

Arturas Meskauskas,[1] Jennifer L. Baxter,[1] Edward A. Carr,[2] Jason Yasenchak,[2] Jennifer E. G. Gallagher,[3] Susan J. Baserga,[3] and Jonathan D. Dinman[1]*

Department of Cell Biology and Molecular Genetics, University of Maryland, College Park, Maryland, 20742[1]; Graduate School of Biomedical Sciences, Rutgers University and The University of Medicine and Dentistry of New Jersey-Robert Wood Johnson Medical School, Piscataway, New Jersey, 08854[2]; and Department of Molecular Biophysics and Biochemistry, Yale School of Medicine, New Haven, Connecticut 06520-8024[3]

Received 3 October 2002/Returned for modification 25 November 2002/Accepted 12 December 2002

***mof6-1* was originally isolated as a recessive mutation in *Saccharomyces cerevisiae* which promoted increased efficiencies of programmed −1 ribosomal frameshifting and rendered cells unable to maintain the killer virus. Here, we demonstrate that *mof6-1* is a unique allele of the histone deacetylase *RPD3*, that the deacetylase function of Rpd3p is required for controlling wild-type levels of frameshifting and virus maintenance, and that the closest human homolog can fully complement these defects. Loss of the Rpd3p-associated histone deacetylase function, either by mutants of *rpd3* or loss of the associated gene product Sin3p or Sap30p, results in a delay in rRNA processing rather than in an rRNA transcriptional defect. This results in production of ribosomes having lower affinities for aminoacyl-tRNA and diminished peptidyltransferase activities. We hypothesize that decreased rates of peptidyl transfer allow ribosomes with both A and P sites occupied by tRNAs to pause for longer periods of time at −1 frameshift signals, promoting increased programmed −1 ribosomal frameshifting efficiencies and subsequent loss of the killer virus. The frameshifting defect is accentuated when the demand for ribosomes is highest, suggesting that rRNA posttranscriptional modification is the bottleneck in ribosome biogenesis.**

A growing yeast cell must produce ~2,000 ribosomes per min, each of which must be able to translate mRNAs with extremely high accuracy (reviewed in reference 80). In the model organism *Saccharomyces cerevisiae*, the coordinate expression of 137 ribosomal protein (RP) genes and ~150 rRNA genes is required to synthesize the appropriate levels of the 78 proteins and four species of rRNAs that are used to form mature small (40S) and large (60S) ribosomal subunits. Although a premium has been placed on fidelity of the translational apparatus, a number of examples have been described where translating ribosomes are directed to shift translational reading frames in response to specific *cis*-acting mRNA signals. As exceptions to the general rule, such programmed ribosomal frameshifting (PRF) events provide a convenient means to probe the molecular mechanisms underlying ribosome structure and function relationships as well as a unique window into the translation elongation cycle. In addition, PRF has been shown to play a critical role in the morphogenesis of RNA viruses (reviewed in reference 18). Given that human immunodeficiency virus and many other animal and plant pathogens utilize PRF, an understanding of the molecular mechanisms that govern PRF can also provide insight into rational antiviral therapeutic strategies.

The most common programmed ribosomal frameshifts involve slippage of the translational complex by 1 nucleotide in the 5′ (−1) or 3′ (+1) direction. A typical −1 PRF signal is composed of two *cis*-acting elements, a heptameric "slippery site" followed by a strong secondary mRNA structure such as a pseudoknot (reviewed in references 4, 24, and 28). The mRNA structure induces an elongating ribosome to pause, positioning the A and P site tRNAs over the slippery site (47, 65, 72). At a given frequency (depending on the viral system), the ribosome is directed to slip back a single base in the 5′ direction. After the slip, the nonwobble bases of the ribosome-bound tRNAs can base pair with the −1 frame codons, and translation continues in the −1 frame (37, 38). We have made extensive use of the yeast killer virus system to probe the genetics, molecular biology, and biochemistry of programmed −1 ribosomal frameshifting (reviewed in references 12 and 18). The 4.6-kb double-stranded RNA (dsRNA) genome of the L-A virus contains two open reading frames (ORFs), which are organized 5′ *gag* and 3′ *pol* with respect to the translation start codon. The *gag* gene encodes the major viral structural protein, and *pol* encodes a multifunctional enzyme that has RNA-dependent RNA polymerase (Pol) activity as well as a viral RNA packaging domain (27, 35). Host cell ribosomes translate the L-A mRNA, producing the 0 frame-encoded Gag and −1 PRF-encoded Gag-Pol fusion proteins (15, 74). The 1.8- to 1.6-kb dsRNA genome of the M_1 satellite virus of L-A is both replicated and encapsidated in L-A-encoded viral particles and encodes a secreted toxin and an immunity factor that allows virus-infected cells to kill uninfected cells (reviewed in references 5 and 81). Generally, changing the frequency or efficiency of −1 PRF at the L-A frameshift signal promotes loss of the M_1 virus (reviewed in references 12 and 18).

There are a number of parameters that can influence the ability of ribosomes to maintain translational reading frame

* Corresponding author. Mailing address: Department of Cell Biology and Molecular Genetics, University of Maryland, College Park, MD 20742. Phone: (301) 405-0918. Fax: (301) 314-9489. E-mail: jd280@umail.umd.edu.

TABLE 1. Yeast strains used in this study

Strain	Description	Source
5X47	Standard diploid killer tester	J. D. Dinman
JD758	3164 *MAT***a** *kar1-1 arg1* [L-AHN M^1]	J. D. Dinman
JD469-2D	*MAT*α *leu2-1*::pJD85 *ura3 his4 mof6-1*	J. D. Dinman
JD932D	*MAT***a** *ade2-1 trp1-1 ura3-1 leu2-3,112 his3-11,15 can1-100* [L-AHN M_1]	J. D. Dinman
LNY95	*MAT***a** *ura3*-SK1 *leu2-hisG trp1-hisG lys2*-SK1 *ho*::*LYS2 ade3-210S*	L. Neigeborn
JD972A	*MAT***a** *ura3*-SK1 *leu2-hisG trp1-hisG lys2-SK1 ho*::*LYS2 ade3-210SPEX6*::*URA3*	This study
YMH171	*MAT*α *ura3-52 leu2-3,112 his3 trp1*Δ	M. Hampsey
YMH265	*MAT*α *ura3-52 leu2-3,112 his3 trp1*Δ *sin3*::*LEU2*	M. Hampsey
YMH270	*MAT*α *ura3-52 leu2-3,112 his3 trp1*Δ *rpd3*::*LEU2*	M. Hampsey
YMH277	*MAT*α *ura3-52 leu2-3,112 his3 trp1*Δ*sap30*::*LEU2*	M. Hampsey
AJ82	*MAT*α *trp1 leu2 ura3 his4 UME6*	A. Vershon
AJ82 11-2	*MAT*α *trp1 leu2 ura3 his4 ume6-11-2*	A. Vershon
AJ82 66-2	*MAT*α *trp1 leu2 ura3 his4 ume6-66-1*	
AJ82 77-2	*MAT*α *trp1 leu2 ura3 his4 ume6-72-2*	

(reviewed in reference 31). These include changes in the residence time of ribosomes at a particular PRF signal and the precise step of the elongation cycle when such a kinetic change might occur, changes in the stabilities of ribosome-bound tRNAs due to alterations in intrinsic ribosomal components such as RPs and rRNAs, and defects in the abilities of ribosomes to recognize and correct errors. In combination with the current high-resolution structural understanding of ribosomes, studies of PRF are leading to new insights into ribosome structure-function relationships and also have utility for the identification of new targets for antiviral agents.

In the course of this study, alleles of several yeast chromosomal genes that specifically increase −1 PRF efficiency were characterized. Nine chromosomal *mof* (maintenance of frame) mutants have been described previously (19–21), and alleles of other translation-associated genes with Mof^- phenotypes have also been identified (3, 16, 50, 56, 59, 64). Concomitant loss of the killer virus occurs in strains harboring the *mof1-1*, *mof2-1*, *mof4-1*, *mof5-1*, and *mof6-1* alleles (20). *MOF2* and *MOF4* are allelic to *SUI1* (11) and *UPF1* (12), respectively. This work focuses on the cloning and characterization of *MOF6*. We show that *mof6-1* is an allele of *RPD3*, the well-characterized histone deacetylase that is involved in transcriptional activation and silencing (67, 68). The defect is dependent on the histone deacetylase activity of the gene product and can be rescued by the human homolog, HDAC1. Expression of the mutant *rpd3* alleles results in delayed exit from lag-phase growth and premature auxotrophic shift, suggestive of a defect in carbon source mobilization and utilization. The frameshifting defect is most pronounced in early log phase, when demand for newly synthesized ribosomes is greatest. The demonstration that deletion of either the *SIN3* or the *SAP30* gene (69) also promoted frameshifting and virus maintenance defects suggests a heterochromatin-associated defect. Processing of the 35S precursor rRNA was delayed in isogenic strains harboring mutant *rpd3* alleles and in cells containing gene knockout alleles of *SIN3* and *SAP30*. In actively growing cells, this delay in rRNA processing appears to be the primary event that results in a 60S ribosomal subunit biogenesis defect. The resulting unstable ribosomes have specific aminoacyl (aa)-tRNA binding defects that result in decreased peptidyltransferase activities. This in turn results in decreased rates of peptidyl transfer, allowing ribosomes stalled at the −1 PRF signal more time to slip. We suggest that the heterochromatin-associated Rpd3p/Sin3p/Sap30p complex (69) could be physically involved in helping to coordinate a very early and critical step in the ribosome biogenesis program. Alternatively, elimination of the function of this complex may result in repression of synthesis of the snoRNAs responsible for modification of bases in the large-subunit rRNA that are associated with the A site, resulting in the observed phenotypic defects.

MATERIALS AND METHODS

Strains, oligonucleotides, sequencing, media, enzymes, and genetic methods. The *S. cerevisiae* strains used in this study are presented in Table 1. Oligonucleotides were synthesized and purchased from IDT and are listed in Table 2. DNA sequence analysis was performed by the Robert Wood Johnson Medical School DNA Synthesis and Sequencing Laboratory. *Escherichia coli* strains DH5α and MV1190 were used to amplify plasmids, and *E. coli* transformations were performed by using the standard calcium chloride method as described previously (60). Yeast were transformed by using the alkali cation method (36). YPAD, YPG, SD, synthetic complete medium (H−), and 4.7MB plates for testing the killer phenotype were used (82). Cytoduction of L-A and M_1 viruses from strain JD758 into rho-o strains was done as previously described (20). Restriction enzymes were obtained from Promega, MBI Fermentas, and Roche. T4 DNA ligase and T4 DNA Pol were obtained from Roche, and precision *Taq* Pol was obtained from Qiagen. Radioactive nucleotides were obtained from NEN. Michael Hampsey generously provided the *rpd3*Δ, *sin3*Δ, and *sap30*Δ yeast strains, and the transcription derepression-defective *ume6* strains were a gift from Andrew Vershon.

To monitor temperature sensitivity, cells were grown to saturation and equal numbers, spotted on selective medium, and grown at either the permissive temperature (30°C) or the restrictive temperature (37°C) for 3 days. Lack of growth or severely reduced growth was indicative of temperature sensitivity. Similarly, 10-fold serial dilutions of cells were spotted onto medium containing sparsomycin (5 μg/ml), anisomycin (5 μg/ml), or paromomycin (800 μg/ml) for monitoring of sensitivities to these drugs. To monitor sensitivity to cycloheximide, cells were grown to saturation at an optical density at 595 nm (OD_{595}) of 0.1 and were spread on selective medium. A sterile filter disk containing 100 ng of cycloheximide was placed in the center of each plate. Cells were grown for 3 days, and zones of growth inhibition were measured.

The killer virus assay was done by replica plating *S. cerevisiae* colonies onto 4.7MB plates (82) with a freshly seeded lawn of strain 5X47 (0.5 ml of a suspension at 1 U of OD_{550} per ml per plate). After 2 to 3 days at 20°C, killer activity was observed as a zone of growth inhibition around the killer colonies. dsRNAs of L-A and M_1 viruses were prepared as described previously (26, 46) and separated by electrophoresis through 1.0% nondenaturing agarose gels and visualized by ethidium bromide staining. RNA blotting was used as previously described (20) to monitor the abundance of L-A and M_1 dsRNAs.

Plasmid and strain constructs, PRF, and transcriptional derepression assays. A YCp50-based *S. cerevisiae* genomic library was purchased from the American Type Culture Collection (58). The genomic clone that complemented the *mof6-1*

TABLE 2. Primers used in this study

Primer	Sequence
Sequencing primers	
Reverse primer	5′ TTCACACAGGAAACAG 3′
Universal primer	5′ GTAAAACGACGGCCAGT 3′
RPD3 sequencing oligonucleotide 1	5′ GCCGCATAGAATAAGAATGG 3′
RPD3 sequencing oligonucleotide 2	5′ GGTTCAAACACAGATCTATACG 3′
RPD3 sequencing oligonucleotide 3	5′ GCTGTCGTGTTACAGTGTGG 3′
PCR primers[a]	
1 (forward primer *Xho*I)	5′ CCCCCTCGAGTGTCCCATATTTTGCCTTG 3′
2 (reverse primer *Pst*I)	5′ CCCCCTGCAGTTGTCATGCTCAACATGTAGG 3′
3 (forward primer *Kpn*I)	5′ CCCCGGTACCTCATGTAGCCAATTGCTACAC 3′
4 (reverse primer *Sal*I)	5′ CCCCGTCGACTCAAAATTAGCTCTCACCGC 3′
5 (forward primer *Xho*I)	5′ CCCCCTCGAGTCAAATAAGTTGCATTGTTCG 3′
6 (reverse primer *Pst*I)	5′ CCCCCTGCAGTCAAAAGCTATCCTGGCAGA 3′
Oligonucleotide H151A[b]	5′ GCTTCCGATTTTTTTGCAGCATGCAAACCACCCGC 3′

[a] Primers 1 and 2, 3 and 4, and 5 and 6 were used to clone *rpd3*, *PEX6*, and *AAD14* alleles, respectively, from genomic DNA.
[b] Mutagenized bases are underlined.

ts$^-$ phenotype was given the name pJD155. Subclones of pJD155 were generated by partial digestion with *Eco*RI and self ligated by using a Roche rapid ligation kit. The pRS series of plasmids have been previously described (9, 63). Full-length *RPD3*, *PEX6*, and *AAD14* genes were amplified from genomic DNA from JD932D by PCR using the oligonucleotide primers 1 and 2 (*rpd3* alleles), 3 and 4 (*PEX6*), and 5 and 6 (*AAD14*) (Table 2) and cloned into pRS314 and pRS316 and were then designated pRPD3, pPEX6, and pAAD14, respectively. The *mof6-1* allele was amplified from genomic DNA obtained from strain JD469-2C by using primers 1 and 2. PCRs using the oligonucleotide primers 1 and 2 were carried out under the following conditions: denaturation of dsDNA for 30 s at 95°C, annealing at 48°C for 45 s, and elongation for 4 min. PCR products were purified by using a Qiagen kit, digested with *Xho*I and *Pst*I, and ligated into pRS314 or pRS316 (63). PCRs using oligonucleotide primers 3 and 4 (*PEX6*) or 5 and 6 (*AAD14*) were carried out under the following conditions: denaturation of dsDNA for 30 s at 95°C, annealing for 45 s at 48°C, and elongation for 6 min. PCR products were purified by using a Qiagen kit, digested with *Kpn*I and *Sal*I (*PEX6*) or *Xho*I and *Pst*I (*AAD14*), and ligated into pRS314. To make pHDAC1, the 1.5-kb *Bam*HI fragment containing the HDAC1 cDNA (a generous gift from S. L. Schreiber) was excised from pBJ5/HDAC1-F (70) and inserted into *Bam*HI-digested pG-1 (61), thus placing the human gene under control of the constitutive yeast *PGK1* promoter. The synthetic oligonucleotide H151A (Table 2) was used to create pH151A by use of standard methods (43). Subcloning *PEX6* into pRS306 (63) generated plasmid pPEX6, which was used to integrate *URA3* into the *PEX6* locus of yeast strain LNY95. pRPD3, pSIN3, and pSAP30 were generous gifts from M. Hampsey.

Plasmids p−1 and p0, which were used to monitor PRF, have been described previously (73). Briefly, in these plasmids, transcription is driven from the yeast *PGK1* promoter into an AUG translational start site. The *E. coli lacZ* gene serves as the enzymatic reporter, and transcription termination utilizes the yeast *PGK1* transcriptional terminator. In the p0 plasmids, *lacZ* is in the 0 frame with respect to the translational start site, and measurement of β-galactosidase activity generated from cells transformed with these plasmids serves to represent the 0-frame controls. In the p−1 series, *lacZ* is in the −1 frame with respect to the translational start site and is 3′ of the L-A programmed −1 ribosomal frameshift signal such that β-galactosidase can only be produced as a consequence of a programmed −1 ribosomal frameshift. The efficiency of PRF was calculated by determining the ratio of β-galactosidase activity produced by cells harboring p−1 to the β-galactosidase activity produced by cells harboring p0 and multiplying this ratio by 100. All assays were performed in triplicate.

Plasmids pAV73 and pAV138 were used to monitor transcriptional derepression in cells harboring alleles of *RPD3* (76). pAV73 is a *URA3* 2μm *CYC-LacZ* fusion reporter plasmid that is used as a control to establish a baseline. PAV138 contains a URS1 site from the *HOP1* promoter cloned into the *Xho*I site of pAV73. It represses *lacZ* expression in a Ume6p/Sin3p/Rpd3p-dependent manner. The pAV73/pAV138 ratios of β-galactosidase activities were used to calculate the ability of the *RPD3* variants to derepress *lacZ* reporter gene transcription as previously described (76). All assays were performed in triplicate.

In vivo [^{35}S]methionine incorporation. Labeled methionine incorporation assays were performed as previously described (7). Briefly, isogenic *rpd3*Δ strains containing wild-type pRPD3 or p*mof6-1* were grown in 30 ml of medium lacking methionine and tryptophan at 30°C to an OD_{595} of 1.0. Unlabeled methionine was added to a concentration of 50 μM, and [^{35}S]methionine and [^{35}S]cysteine (Expre^{35}S^{35}S Label; NEN Life Science Products) were added to each culture to final specific activities of 1.1 μCi/ml. Samples were harvested at 0 min and at 15-min intervals for 60 min. Incorporation of the [^{35}S] labels was monitored by cold trichloroacetic acid (TCA) precipitation. For each time point, 1.2-ml aliquots were harvested, from which 0.2 ml was used to determine the OD_{595} of the cultures. One milliliter of ice-cold 20% TCA was added to the remaining 1 ml of each aliquot, incubated on ice for 10 min, heated to 70°C for 20 min, and filtered through prewet Whatman GF/C filters. Filters were sequentially washed with 10 ml of ice-cold 5% TCA and 10 ml of 95% ethanol and dried, and the radioactivity of samples was determined by scintillation counter. All time points were taken in triplicate.

Pulse-chase labeling of rRNA. Pulse-chase labeling with L-[methyl-^{3}H]methionine was carried out on the isogenic wild-type, *mof6-1*, *rpd3*Δ, *rpd3-H151A*, *sin3*Δ, and *sap30*Δ strains as previously described (23, 45). Twenty thousand counts per minute per sample were resolved on a 1.2% formaldehyde-agarose gel. Labeled RNAs were transferred to a zeta probe membrane (Bio-Rad), sprayed with En^{3}Hance (Dupont), and exposed to X-ray film.

Polysome and two-dimensional NEPHGE analyses. For polysome analyses, cytoplasmic extracts, prepared as described by Baim et al. (2), were fractionated on 7 to 47% sucrose gradients buffered with 50 mM Tris-acetate (pH 7.4), 50 mM NH_4Cl, 12 mM $MgCl_2$, and 1 mM dithiothreitol (DTT). Gradients were centrifuged in an SW41 rotor at 40,000 rpm for 135 min at 4°C, fractionated, and analyzed by continuous monitoring of A_{254} (55). For nonequilibrium pH gradient gel electrophoresis (NEPHGE) analyses, 40S and 60S ribosomal subunits were separated by ultracentrifugation through a 7 to 27% sucrose gradient in the presence of 500 mM EDTA. Purified ribosomal subunits (≈195 μg/sample) were separated by NEPHGE (pH gradient of 3.5 to 11.5% in the first dimension and 12.5% polyacrylamide separating gel in the second dimension) and were visualized by silver staining by the Kendrick Laboratories (Madison, Wis.).

Preparation of tRNAs and of donor and acceptor fragments. Yeast tRNAs were charged with [^{14}C]phenylalanine as previously described (32, 50). Briefly, a 400-μl reaction mix composed of 200 μg of yeast tRNA (Sigma), 25 mM Tris-HCl (pH 7.5), 20 mM $MgCl_2$, 10 mM ATP, 50 nmol of phenylalanine (313 mCi/mmol; NEN), and 50 μl of aa-tRNA synthetase (9 U/ml; Sigma) was incubated for 25 min at 37°C. After addition of 40 ml of 3 M sodium acetate (pH 5.0), the mixture was extracted twice with an equal volume of water-saturated phenol and once with chloroform. It was then precipitated with 2.5 volumes of ethanol at −20°C for 1 h. After centrifugation for 10 min, the pellet was resuspended in 50 ml of 2 mM potassium acetate (pH 5.0). [^{14}C]Phe-tRNA^{Phe} was separated from uncharged tRNAs by using DEAE Sephadex as previously described (57). Acetylation of charged tRNAs was performed as previously described (30). Briefly, [^{14}C]Phe-tRNA^{Phe} was resuspended in 200 μl of 0.2 M sodium acetate

(pH 5.0), followed by addition of 2.5 μl of acetic anhydride. After a 1-h incubation on ice, another 2.5 μl of acetic anhydride was added, and incubation at 0°C was done for an additional hour. The tRNA was precipitated by addition of 2.5 volumes of ethanol. The [^{14}C]Phe-tRNA^{Phe} and acetyl-[^{14}C]Phe-tRNA^{Phe} were subsequently digested with 500 U of RNase T1 in 200 μl of 0.3 M sodium acetate (pH 5.0) for 1 h at 37°C, and the reaction mixtures were purified by using DEAE Sephadex as previously described (57). The resulting A site-specific [^{14}C]Phe-CACCA (acceptor) and P site-specific acetyl-[^{14}C]Phe-CACCA (donor) fragments were used as substrates for the tRNA fragment binding assays.

Purification of ribosomes and tRNA binding assays. Salt-washed ribosomes were purified as previously described (48, 50). Briefly, yeast cells were grown in 0.5 liters of YPAD overnight, collected by centrifugation, and washed twice with buffer A (20 mM Tris-HCl [pH 7.5], 10 mM $MgCl_2$, 1 mM DTT, 0.1 mM EDTA, 0.25 M sucrose). The cell pellet was suspended in 20 ml of buffer A, 30 g of glass beads (0.45-mm diameter) were added, and cells were disrupted by vortexing. The yeast lysate was centrifuged twice for 15 min at 15,000 rpm in a Sorvall S34 rotor, and the supernatant was pelleted at 100,000 × *g* for 3 h. The pellet was suspended in 6 ml of buffer B (20 mM Tris-HCl [pH 7.5], 10 mM $MgCl_2$, 1 mM DTT, 0.1 mM EDTA, 0.25 M sucrose, 0.5 M KCl) and placed on a cushion of 3 ml of buffer C (20 mM Tris-HCl [pH 7.5], 10 mM $MgCl_2$, 1 mM DTT, 0.1 mM EDTA, 1 M sucrose, 0.5 M KCl). After centrifugation at 50,000 rpm for 4 h (SW55 Ti), the pellet was dissolved in 1 ml of buffer A. After a clarifying spin for 1 min in a microcentrifuge, OD_{260} readings were taken (1 A_{260} unit = 19 pmol of ribosomes [1]). The protein content of ribosomes was also estimated by using protein assay reagent (Bio-Rad). Ribosomes were suspended in buffer A at a concentration of 4 pmol/μl and stored at −70°C.

The whole-tRNA and tRNA fragment binding assays were performed by following a modification of previously published protocols (32, 50). Briefly, ribosomes (400 pmol) were incubated with 800 pmol of whole tRNAs or donor or acceptor fragments in 500 μl of a buffer containing 70 mM Tris-acetate (pH 7.2), 40 mM magnesium acetate, 0.4 M potassium acetate, and 50 mM NH_4Cl. Ethanol was added to a final concentration of 30%, and 20-μl aliquots were taken during the time course at 24°C. Samples were diluted to 1 ml with cold buffer (50 mM Tris-HCl [pH 7.2], 0.4 M KCl, 40 mM $MgCl_2$, 30% ethanol), immediately precipitated onto a Millipore filter, washed with 1 ml of the dilution buffer, and counted in a scintillation counter. The reaction mix without ribosomes was used as the control. All assays were performed in triplicate.

Puromycin reaction with tRNA fragments. Puromycin reactions were performed as previously described (14), with slight modifications. Ribosomes (20 pmol) were incubated with 5 pmol of CACCA[^{14}C]AcPhe (682 dpm/pmol) in 300 μl of PR buffer (25 mM HEPES-KOH [pH 7.4], 135 mM NH_4Cl, 250 mM KCl, 20 mM $MgCl_2$, 33% EtOH) at 0°C for 10 min. Puromycin was added to final concentrations of 1 mM, and reaction mixes were incubated on ice. At indicated time points, 50-μl aliquots were taken, and reactions were stopped by the addition of equal volumes of a 0.3 M sodium acetate solution saturated with $MgSO_4$. Puromycin was extracted with 1 ml of ethyl acetate, and the radioactivity was determined by liquid scintillation counting. In all of the experiments, controls were analyzed in the absence of puromycin to determine the nonspecific extraction of CACCA[^{14}C]AcPhe. Control values (generally less than 2%) were subtracted from the values obtained in the presence of puromycin.

RESULTS

***mof6-1* is an allele of *RPD3*.** The ts$^-$ phenotype of *mof6-1* cells (20) provided a simple selective trait for the cloning of the wild-type gene. *mof6-1* cells (JD469-2D) transformed with a YCp50-based genomic library (58) were replica plated to selective medium and subsequently shifted to nonpermissive temperature (37°C). Approximately 1.2×10^4 colonies were screened (4.8 genome equivalents), and three colonies that grew at the restrictive temperature were isolated. Positive plasmids were rescued from yeast into *E. coli*, and reintroduction into *mof6-1* cells confirmed their abilities to confer growth at the nonpermissive temperature. The inserts in all of the genomic clones were approximately 13 kb in length, and sequence analysis mapped them all to the same region of chromosome XIV. One of the genomic clones, pJD155, was used for the subsequent characterization of *MOF6*. Meiotic linkage analysis was used to ascertain whether pJD155 harbored *MOF6* as opposed to a second site suppressor. The *URA3* gene was inserted into the *PEX6* locus of a *MOF6 ura3* strain (JD972A) (Fig. 1A), providing a scorable phenotype for genetic linkage analyses. Diploid cells (JD972A × JD469-2D) were sporulated, and the genotypes of 26 tetrads were determined. All of the tetrads scored as parental ditypes, i.e., 2:2 segregation of Ura$^+$ ts$^+$:Ura$^-$ ts$^-$. The absence of crossover events demonstrates tight genetic linkage between *MOF6* and the site of *URA3* integration (*PEX6*), confirming that *MOF6* was present in the yeast genomic DNA insert of pJD155.

Partial restriction analysis of pJD155 revealed four *Eco*RI restriction fragments, which were designated A, B, C, and D based on their relative electrophoretic mobilities (Fig. 1A). All subclones generated from partial *Eco*RI digestion which did not contain the B fragment were unable to complement the temperature-sensitive phenotype (e.g., pJD155.CAD [Fig. 1A]). Sequence analysis revealed that the B fragment contained *RPD3*. To determine whether *MOF6* is *RPD3* or whether the B fragment contained other genetic information required for transcription initiation or 3′-end formation of flanking genes, clones of the individual ORFs that were present on the genomic clone were generated by PCR as described in Materials and Methods (Fig. 1A). *mof6-1* cells harboring either pJD155 or pRPD3 but not pPEX6 or pAAD14 were able to grow at restrictive temperatures (Fig. 1). Furthermore, an *RPD3* clone generated from *mof6-1* genomic DNA, p*mof6-1*, was not able to complement the ts$^-$ phenotype (Fig. 1), confirming that *RPD3* is both necessary and sufficient to complement the *mof6-1* ts$^-$ phenotype.

PRF assays were used to examine whether pRPD3 could complement the *mof6-1* frameshifting defect. The frameshift test plasmids p−1 and the 0-frame control p0 were introduced into *mof6-1* cells harboring pRPD3, pPEX6, pAAD14, or p*mof6-1*, and the effects on −1 PRF were assayed. Whereas introduction of the wild-type gene pRPD3 restored −1 PRF efficiencies to wild-type levels (approximately 2.0%), frameshifting efficiencies remained elevated in cells harboring the other clones (Fig. 1A). Sequence analysis of *mof6-1* clones isolated from three independent PCRs revealed the presence of a single base transition, G1218A, corresponding to a change at the amino acid level of aspartic acid to asparagine (GAT → AAT) at position 407, approximately 30 residues from the C terminus of the protein (data not shown). A ClustalW analysis (71) revealed that that yeast has an acidic residue at this position while the *RPD3* homologs from humans, mice, and *Arabdopsis* contain the basic arginine, suggesting that there may be a requirement for a charged residue in this environment. Unfortunately, the lack of structural information pertaining to this region of the protein precludes any further speculation on the functional role of this amino acid residue.

Two additional plasmid-borne *rpd3* alleles were constructed for further study. Since the *mof6-1* mutation did not occur in the putative deacetylation motif (41), we constructed an allele in this domain by changing the histidine at position 151 to an alanine residue (pH151A), which has previously been shown to nearly eliminate Rpd3p deacetylase activity (40). In addition, since HDAC1 is the most homologous to *RPD3* among the at least seven different human histone deacetylases (70, 79), we used a clone in which transcription of the human HDAC1 cDNA was driven from the yeast *PGK1* promoter (pHDAC1).

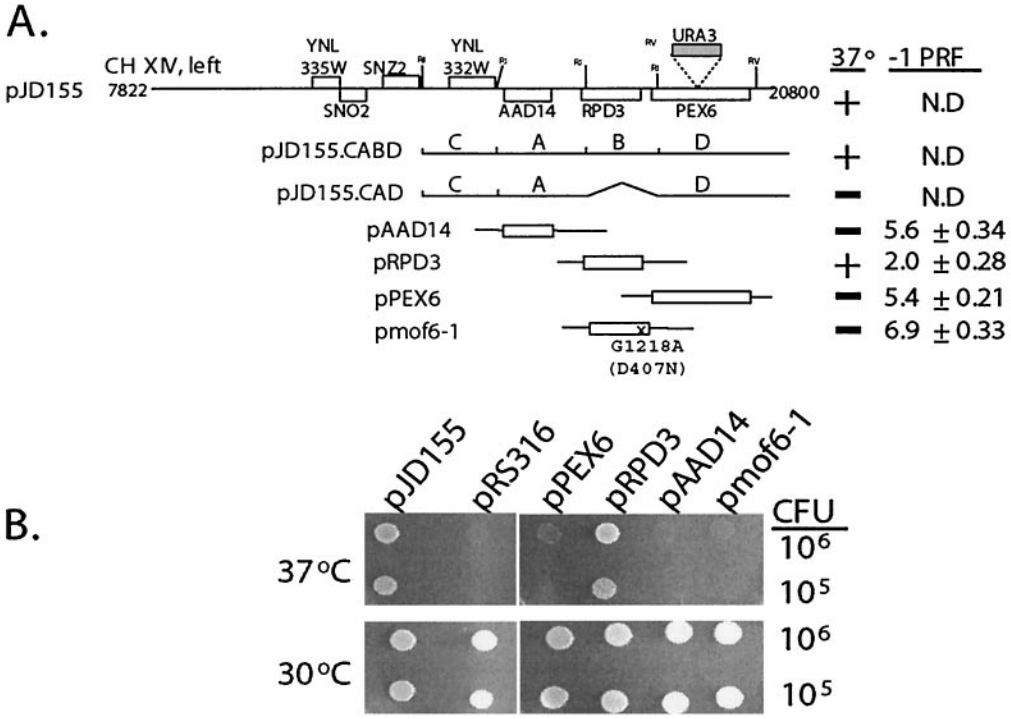

FIG. 1. *mof6-1* is an allele of *RPD3*. (A) Cloning of *MOF6*. At the top is the schematic representation of the ≈13-kb insert isolated from the YCp50 plasmid library (pJD155). Locations of all of the intact ORFs contained in this clone are represented as boxes. The *URA3* gene is shown with a shaded box and the location of its insertion into *PEX6* in strain JD972A is indicated. The subclones of the plasmid pJD155 and of PCR-generated clones of *AAD14*, *RPD3*, *PEX6*, and the *mof6-1* allele of *RPD3* are indicated at left, and their effects on growth and −1 ribosomal frameshifting efficiency (−1 PRF) are shown at right. The molecular lesion in the *mof6-1* allele, a G-to-A transition at position 1218 of the coding sequence, is shown. This results in a change of aspartic acid to asparagine at amino acid 407. N.D, not determined; A, B, C, and D, the four *Eco*RI restriction fragments revealed by partial restriction analysis of pJD155 (see Results). (B) Complementation of the temperature-sensitive phenotype by *RPD3*. *mof6-1* strains (JD469-2D) harboring the indicated clones were spotted onto selective medium and incubated at either the permissive (30°C) or the nonpermissive temperature (37°C) for 4 days.

In order to further characterize *mof6-1* independently of strain-specific background effects, all subsequent experiments were performed with plasmid-borne alleles in the *rpd3*::*LEU2* gene disruption strain YMH270. The resulting isogenic strains were subsequently transformed with the p−1 and p0 frameshift test vectors, and −1 PRF efficiencies were determined. Frameshifting efficiencies were significantly elevated in cells harboring p*mof6-1*, pH151A, and vector alone, while addition of the wild-type gene or the human homolog reduced −1 PRF efficiencies to wild-type levels (Fig. 2A).

To examine the effects of the different *rpd3* alleles on killer virus maintenance, L-A and M_1 viruses were first introduced by cytoplasmic mixing into the *rpd3*Δ strain harboring the wild-type *RPD3* gene on a *URA3*-based *CEN* plasmid, and stable Killer$^+$ colonies were identified. The resulting strain was then transformed with low-copy *TRP1* vectors harboring the different *RPD3* alleles or with a vector control. In parallel to the frameshifting results, increased −1 frameshifting efficiencies correlated with loss of the killer phenotype (Fig. 2B) and with loss of the M_1 satellite virus (Fig. 2C). The results of assays for transcriptional repression (Fig. 2D) and cycloheximide hypersensitivity (data not shown) also demonstrated correlations between these classic *rpd3*-associated phenotypes and defects in programmed −1 ribosomal frameshifting. In addition, introduction of p*mof6-1* into wild-type cells had no effect on −1 frameshifting efficiencies, demonstrating that this does not represent a gain-of-function allele (data not shown). Taken as a whole, these data define *mof6-1*, *rpd3-H151A*, and *rpd3*Δ as *mof*-specific alleles of *RPD3*.

Correlation of growth and frameshifting defects in the *rpd3* mutants. It was observed that the initial appearance and subsequent growth of colonies of *rpd3*Δ cells transformed with the various plasmid-borne mutant alleles of *rpd3* was delayed relative to that of cells containing the wild-type gene. Measurement of growth rates revealed significant quantitative differences. In logarithmic growth, the doubling times of cells harboring either vector alone or the pH151A allele were approximately 1.4-fold longer than that of wild-type controls (doubling time of 3.5 h for cells harboring pRS314 or pH151A versus 2.5 h for cells harboring pRPD3). The growth defect was even greater in *mof6-1* cells, where the doubling time was increased approximately 1.6-fold compared with that of isogenic wild-type cells (4.0 versus 2.5 h). Shifting of cells from stationary-phase growth to fresh medium and subsequent monitoring of cell growth rates revealed that the mutants also exhibited significantly different effects on the quality of growth compared with those of isogenic wild-type controls. Particularly striking was the observation that the mutants remained in lag-phase growth for approximately 2 h longer than did wild-type controls (Fig. 3A), suggestive of a defect in the ability of

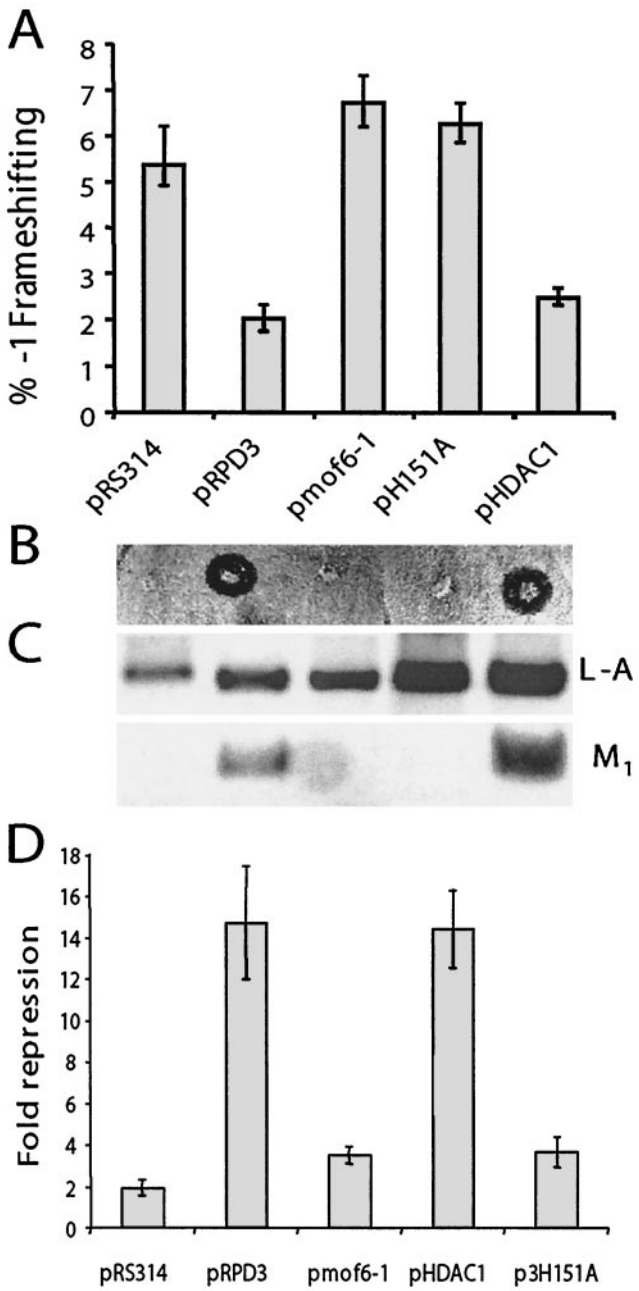

FIG. 2. *RPD3* allele-specific effects on programmed −1 ribosomal frameshifting, killer virus maintenance, transcriptional repression, and sensitivity to cycloheximide. Isogenic *rpd3*Δ cells (YMH270) were transformed with vector alone (pRS314), clones expressing variations of *RPD3* (the wild-type, *mof6-1*, and *H151A* alleles of *RPD3*), or a clone expressing the human homolog, HDAC1. Colonies were selected on synthetic complete medium lacking tryptophan. (A) Functional Rpd3p is required to maintain appropriate levels of programmed −1 ribosomal frameshifting. pRS426-based versions of the frameshift test plasmids p0 and p−1 were introduced into cells, and transformants were selected on medium lacking tryptophan and uracil. Programmed −1 ribosomal frameshifting efficiencies were determined as described in Materials and Methods. All assays were performed in triplicate, and percent errors are indicated with error bars. (B and C) Functional Rpd3p is required to maintain the killer phenotype and the M_1 satellite virus of L-A. The L-A and M_1 viruses were introduced from JD758 into the isogenic strains harboring the various *RPD3* variants by cytoplasmic mixing (20). The killer phenotypes are shown (B). Total nucleic acids were extracted from these cells, separated through a 1.0% nondenaturing agarose gel, denatured in the gel, transferred to a nylon membrane, and hybridized with L-A- and M_1-specific (+) strand probes (C). Hybridizing bands were visualized by autoradiography. The positions of L-A and M_1 are shown. (D) The transcriptional derepression phenotype of the *mof6-1* allele is similar to those of the other loss-of-*RPD3*-function alleles. Derepression phenotypes of the *RPD3* variants were determined as described in Materials and Methods.

the biosynthetic apparatus to respond to the presence of a rich nutrient source. Similarly, the onset of diauxic shift occurred approximately 2 h earlier for cells harboring p*mof6-1* and 1 h earlier for cells harboring pH151A and vector alone than for cells expressing the wild-type gene (Fig. 3A). This result suggests inefficient utilization of carbon source by the mutants.

Given the original translation-associated defect of *mof6-1*, we examined whether these cells exhibited any gross defect in protein synthesis. Rates of incorporation of [^{35}S]-labeled methionine and cysteine into newly synthesized protein in midlogarithmically growing cells were determined as described in Materials and Methods. The results (Fig. 3B) demonstrate that rates of protein synthesis in *mof6-1* cells were approximately 75% of that in wild-type cells.

Previous experiments have demonstrated that programmed −1 ribosomal frameshifting efficiencies remain stable throughout the growth cycle in wild-type cells (15). In light of the effects of the mutants on cell growth, −1 PRF efficiencies were monitored during lag phase, log phase, and after diauxic shift in isogenic *rpd3*Δ cells harboring vector alone, pRPD3, p*mof6-1*, and pH151A. The results of these experiments show that −1 PRF defects were maximized in the mutants in lag phase, becoming less severe as cells progressed through the growth curve (Fig. 3C). The effect was most notable in *mof6-1* cells. The results suggest that the frameshifting defects were maximized in the mutants when demand for newly synthesized ribosomes was the greatest and that −1 frameshifting efficiencies decreased in parallel with the demand for new ribosomes. That no such effect was observed in wild-type cells is in line with the bioeconomic model of regulation of ribosome biosynthesis (80) and suggests a defect in the regulation of ribosome biosynthesis (see below).

Deletion of other genes linked to heterochromatin-associated functions also results in the Mof$^-$ phenotype. Deacetylation of histones by Rpd3p promotes local chromatin condensation, resulting in transcriptional repression of nearby RNA Pol II-transcribed genes (reviewed in reference 10). Although Rpd3p is able to deacetylate histones in vitro, in vivo deacetylation of histones by Rpd3p requires the cofactors. Mutations in any of the components of the Rpd3p/Sin3p/Ume6p repression complex lead to gene-specific derepression of RNA Pol II-regulated genes and concomitant transcriptional activation (33, 40). Conversely, mutations in any of the components of the Rpd3p/Sin3p/Sap30p repression complex lead to the opposite effect, i.e., enhanced transcriptional silencing of RNA Pol II-transcribed genes artificially inserted into heterochromatin contexts (69).

Given the model describing the histone deacetylase complex, if *mof6-1* is acting through either of these complexes, then *sin3* mutants would also exhibit Mof$^-$ phenotypes. Further-

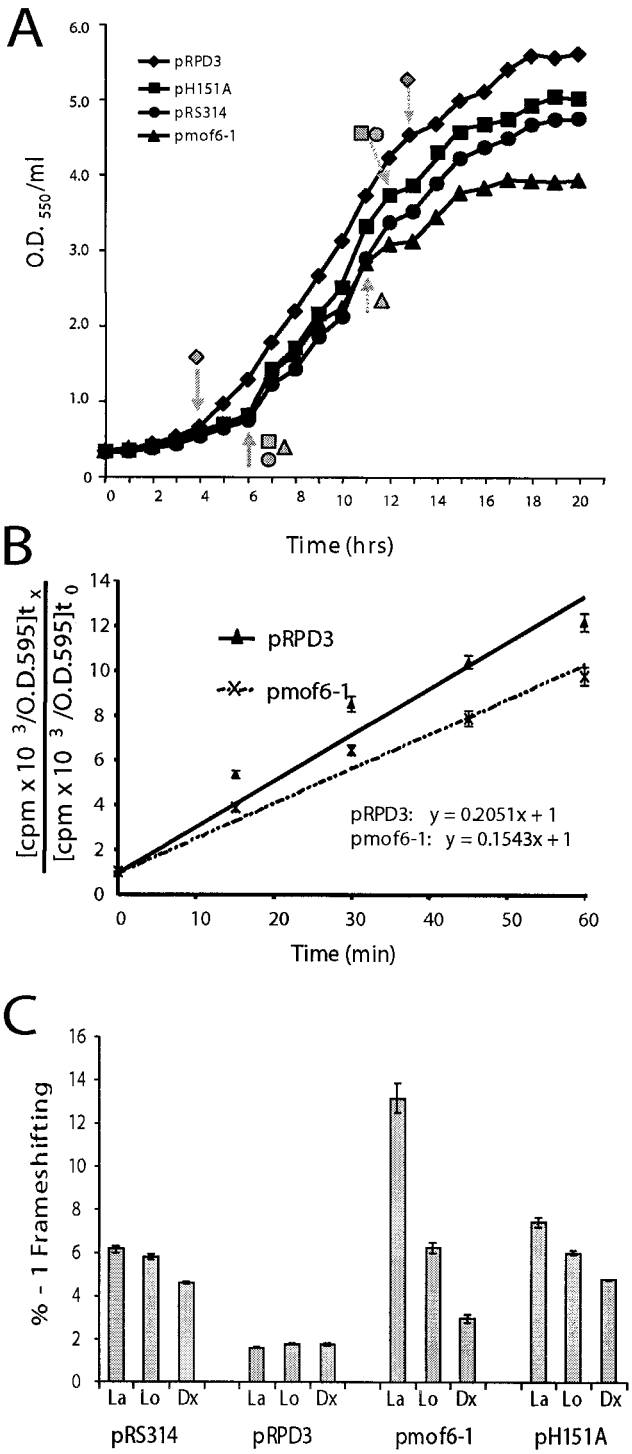

FIG. 3. Correlation of growth and frameshifting defects in the *rpd3* mutants. (A) *rpd3* mutants display delayed exit from lag phase and early entry into diauxic shift. Stationary-phase cultures of isogenic *rpd3*Δ strains harboring vector alone (pRS314) or the indicated plasmid-borne alleles of *RPD3* were diluted into complete synthetic medium lacking tryptophan to 0.3 U of OD_{550}/ml and grown at 30°. At 1-h time points thereafter, aliquots of cells were sampled and OD_{550} readings were determined. Data shown represent the means of each time point through three repetitions of the experiment. Standard deviations were <5%. Solid arrows indicate the approximate point of exit from lag phase, and dotted arrows indicate diauxic shift. (B) Decreased rates of protein synthesis in cells expressing the Mof6-1p form of Rpd3p. [^{35}S]methionine and [^{35}S]cysteine were added to mid-logarithmically growing isogenic *rpd3*Δ strains containing wild-type pRPD3 or p*mof6-1*, and samples were harvested at 0 min and at 15-min intervals for 60 min. Incorporation of the [^{35}S] labels was monitored by cold TCA precipitation as described in Materials and Methods. The data were plotted by using the formula $y = mx + B$, where m is the slope, x is the sample, and B is the y intercept. Rates of protein synthesis correspond to m. All time points were taken in triplicate. (C) Frameshifting defects in the *rpd3* mutants are maximized when demand for ribosomes is greatest. Programmed −1 ribosomal frameshifting efficiencies were determined in isogenic *rpd3*Δ strains harboring vector alone (pRS314) or the indicated plasmid-borne alleles of *RPD3* during the three different phases of cell growth. La, lag-phase growth; Lo, log-phase growth; Dx, after diauxic shift. All assays were performed in triplicate. Error bars denote percent error.

more, if the effect is on a heterochromatin-associated function, e.g., transcription or maturation of rRNAs, then *sap30* mutants should also promote increased −1 PRF efficiencies. Conversely, *ume6* mutants should promote increased −1 PRF efficiencies if the effect is on genes found in euchromatin, e.g., RP genes. Figure 4 shows that deletion of either *SIN3* or *SAP30* resulted in increased −1 PRF efficiencies, while three separate *ume6* alleles did not. The *sin3*Δ and *sap30*Δ strains also had significant killer virus maintenance defects, whereas *ume6* strains were able to stably maintain the killer virus (data not shown). These results demonstrate that (i) the histone deacetylation apparatus is involved in a process that results in a specific translational fidelity defect and (ii) the effect is likely to involve a process in the heterochromatin environment.

Mutation of genes involved in the histone deacetylation apparatus results in 60S ribosomal subunit biogenesis defects. That a defect involving heterochromatin should result in a translational fidelity defect suggested a ribosome biogenesis defect involving rRNA transcription or processing. Given the involvement of the histone deacetylase complex in transcription-associated processes, the effects of these alleles on rRNA transcription and processing were examined by pulsing cells with [^{3}H]methylmethionine, which specifically labels the methylated RNAs, the most abundant of which are those transcribed from the 35S operon. Though no differences were observed with regard to either the rates of 35S pre-rRNA synthesis or its eventual maturation to 18S and 25S rRNAs, the amount of time required for the initial processing step of the 35S pre-rRNA in the mutant cells was delayed by approximately 3 min compared with that for wild-type controls (Fig. 5A). A steady-state analysis revealed that there was no accumulation of any precursors in the mutant cells (data not shown). Polysome analyses of ribosomes isolated from isogenic wild-type, *rpd3*Δ, *mof6-1*, *rpd3-H151A*, *sin3*Δ, and *sap30*Δ strains were suggestive of biogenesis defects in the 60S ribosome subunits, as evidenced by decreased levels of 60S ribosomal subunits, increased areas under the 80S peaks, and decreased polysome peaks (Fig. 5B).

Ribosome biogenesis defects are not due to global defects in RP expression. It has previously been found that defects in specific RPs result in increased PRF efficiencies (50, 56). Thus, one possible explanation for the observed effects could be that these alleles promote altered expression of RPs. To examine this possibility, approximately 200-μg samples of 60S and 40S ribosomal subunits isolated from isogenic wild-type and mu-

tant cells were separated in two dimensions by NEPHGE, and RPs were visualized by silver staining. No gross differences in the staining patterns were observed between wild-type and mutant samples (data not shown). These results demonstrate that the effects of the *rpd3* mutants on PRF and ribosome biogenesis are not due to defects in the synthesis of RPs.

Mutants result in aa-tRNA binding defects. One previously unexplained phenotype of *rpd3* mutants has been their sensitivity to cycloheximide, a translational inhibitor (78). In light of our data showing that these classes of mutants promote a ribosome biogenesis defect specific to 60S subunits, we employed a pharmacogenetic approach using well-characterized antibiotics to investigate the specificity of the defects. Sparsomycin, which increases the affinity of ribosomes for the 3′ (donor) end of peptidyl-tRNAs (34, 39, 51) was used as a P site-specific probe. Anisomycin, which decreases ribosomal affinities for the 3′ (acceptor) ends of aa-tRNAs (6, 29, 62), and paromomycin, which stabilizes binding of near-cognate tRNAs in the decoding center of the small-subunit rRNA (8, 54, 77) served as probes for A site-specific defects. Figure 6A shows that although sparsomycin had no effect relative to the wild type on cells harboring the various *rpd3* alleles (*rpd3*Δ, *mof6-1*, and *rpd3-H151A*) or the *sin3*Δ and *sap30*Δ mutants, all of the mutants were hypersensitive to anisomycin and all but *sap30*Δ were hypersensitive to paromomycin. These data indicate that the translational defect caused by mutations in these genes is specific to the ribosomal A site. To further investigate the biochemical basis for these observations, tRNA binding experiments were performed comparing isogenic wild-type and *mof6-1* ribosomes. Although no differences were observed in the binding of the 3′ ends of either donor or acceptor fragments (data not shown), the binding profiles for intact aa-tRNAs were significantly different (Fig. 6B). Specifically, *mof6-1* ribosomes had decreased initial rates of aa-tRNA binding and had lower overall affinities for aa-tRNAs. In addition, precipitous drop-off in aa-tRNA binding at the 60-min time point suggests that *mof6-1* ribosomes are less stable than their wild-type counterparts.

Ribosomes from *mof6-1* cells have decreased peptidyltransferase activities. It has previously been demonstrated that peptidyl transfer defects can specifically promote increased −1 PRF efficiencies (17, 49). It is possible that a defect in binding of aa-tRNA could result in diminished peptidyltransferase activities. This in turn might enable elongating ribosomes to pause longer at the programmed −1 ribosomal frameshift signal, providing them with more time to shift. To test this hypothesis, we compared the peptidyltransferase activities of ribosomes isolated from isogenic wild-type and *mof6-1* strains by using the puromycin reaction. Figure 6C shows that ribosomes purified from *mof6-1* cells have significantly reduced peptidyltransferase activities compared with that of wild-type controls. These findings illuminate the biochemical basis for the Mof$^-$ phenotypes of these cells.

DISCUSSION

mof6-1 was originally isolated as a recessive mutation in *S. cerevisiae* that promoted increased efficiencies of programmed −1 ribosomal frameshifting and rendered cells unable to maintain the killer virus (20). In the present study, we show that

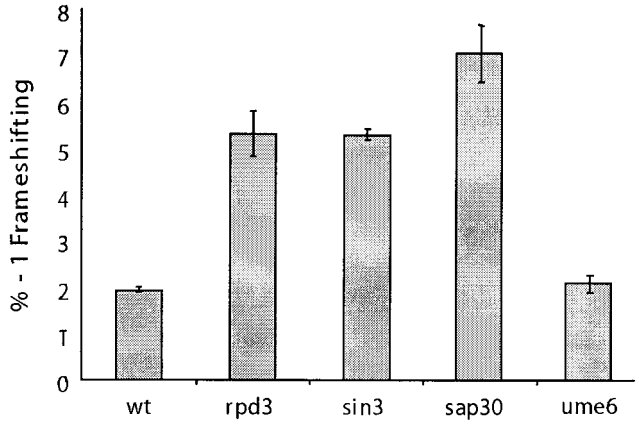

FIG. 4. Deletion of other genes linked to heterochromatin-associated functions also results in frameshifting defects. The frameshift test vectors p0 and p−1 were introduced into isogenic wild-type (YMH171), *rpd3*Δ (YMH270), *sin3*Δ (YMH265), and *sap30*Δ (YMH277) strains, along with four strains harboring different alleles of UME6 (AJ82, AJ82 11-2, AJ82 66-2, and AJ82 77-2), and programmed −1 ribosomal frameshift efficiencies were determined. All assays were performed in triplicate. Error bars denote percent error.

MOF6 is a unique allele of *RPD3*, that it does not represent a gain-of-function allele, and that the deacetylase function of Rpd3p is required for maintenance of wild-type levels of frameshifting and maintenance of the yeast killer virus. The role of *RPD3* in the specific aspect of translational fidelity described here explains the previously noted hypersensitivity to cycloheximide in other alleles of this gene. Furthermore, the ability of the closest human homolog to complement the translational fidelity and virus maintenance defect demonstrates that, in addition to the conservation of its function in the regulation of RNA Pol II transcription, its role in processes involved in the biogenesis of the protein translational machinery has also been preserved.

Specific interactions of the Rpd3p-Sin3p complex with other factors, e.g., Ume6p or Sap30p, have been genetically shown to have differential effects on RNA Pol II-transcribed genes in either euchromatin or heterochromatin environments (69). Our observation that mutants of *RPD3*, *SIN3*, and *SAP30*, but not of *UME6*, affect programmed −1 ribosomal frameshifting and virus maintenance suggests that these translation-associated defects are due to effects in the heterochromatin environment. Though previous work has shown that deletion of *RPD3*, *SIN3*, or *SAP30* promotes repression of RNA Pol II-transcribed reporters that have been artificially inserted into the *RDN1* locus, the fact that there was no quantitative effect on rates of 35S rRNA synthesis argues against the observed effects on ribosome biogenesis and function being a consequence of a simple rRNA transcriptional defect. Rather, we have shown that the defect is a delay at the earliest stage in the 35S pre-rRNA processing program. Since processing of the 35S pre-rRNA is cotranscriptional (25) and since the histone deacetylase complex is known to influence chromatin structure, one possible explanation for our observations could be that a change (or the lack thereof) in the heterochromatin topological environment is perturbing an early function of the apparatus, e.g., the 60S processosome (22), that is required for assembly of the large ribosomal subunit.

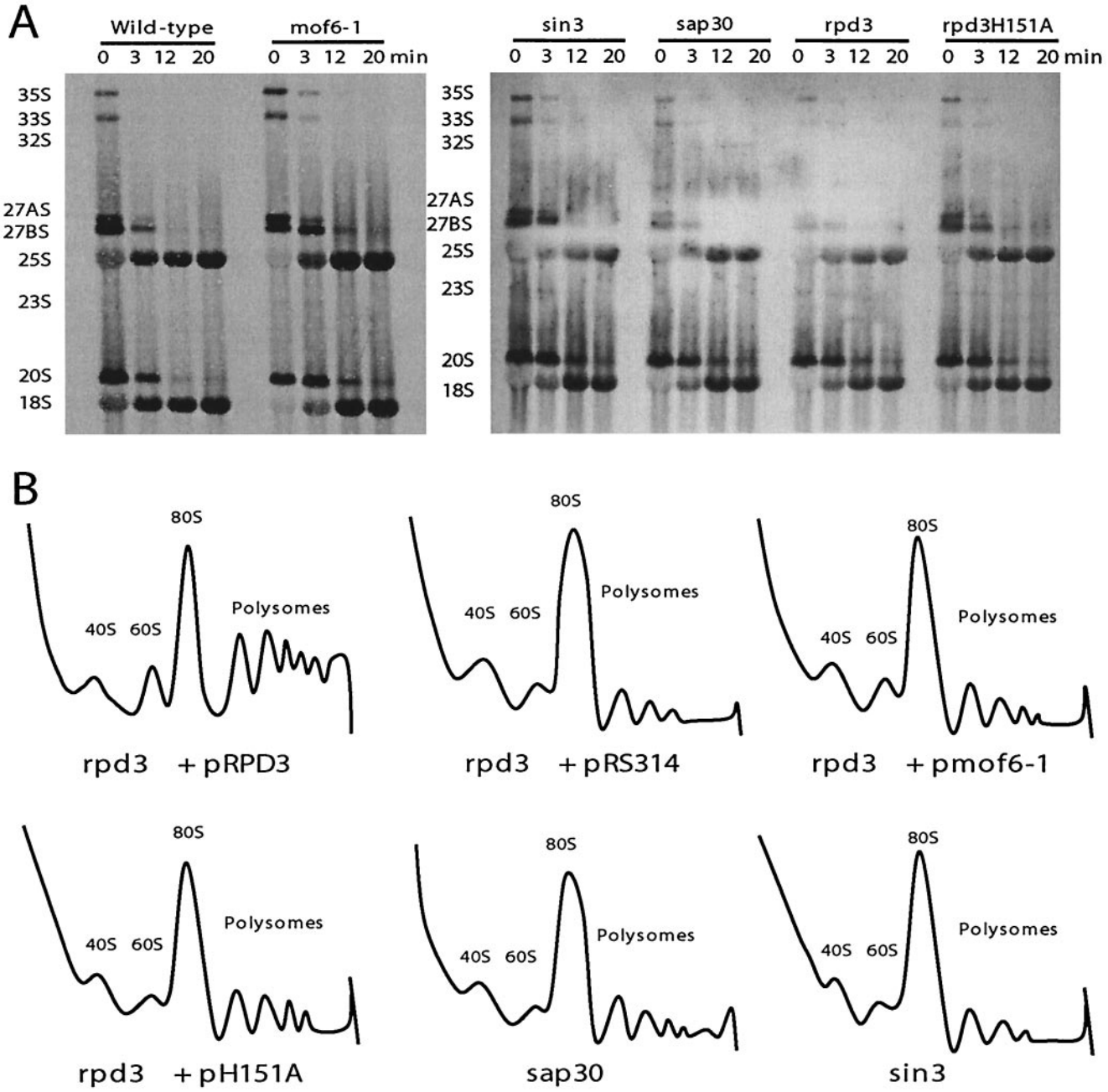

FIG. 5. Mutations of genes involved in histone deacetylation result in ribosome biogenesis defects. (A) Delayed 35S rRNA processing. Pulse-chase labeling with L-[methyl-^{3}H]methionine was carried out on the isogenic wild-type, *mof6-1*, *rpd3*Δ, *rpd3-H151A*, *sin3*Δ, and *sap30*Δ strains as previously described (23, 45). Twenty thousand counts per minute per sample were resolved on a 1.2% formaldehyde-agarose gel. Labeled RNAs were transferred to a zeta-probe membrane, sprayed with En^{3}Hance, and exposed to X-ray film. (B) 60S ribosomal subunit biogenesis and polysome defects. Cytoplasmic extracts from isogenic strains were fractionated though sucrose gradients as described in Materials and Methods. Gradients were centrifuged in an SW41 rotor at 40,000 rpm for 135 min at 4°C, fractionated, and analyzed by continuous monitoring of A_{254} (55).

In light of the well-defined steps involved in rRNA maturation (for reviews, see references 42, 44, and 75), our data suggest the possibility that the defect may be at the level of rRNA base modification, e.g., 2′-*O*-ribose methylation and/or pseudouridylation. These types of base modification have been specifically shown to localize to functional regions of the ribosome (13). Of particular interest with regard to the ribosomal A site-specific defect observed here are the large numbers of modified bases clustered in regions of the large-subunit rRNA that are associated with the A site–aa-tRNA interactions and the peptidyltransferase center (reviewed in references 13 and 53). These include (i) the peptidyltransferase center core region; (ii) the region of helix 38 that forms an "A-minor motif" with 5S rRNA (52); (iii) helix 69, which appears to form an important bridge between the aa- and peptidyl-tRNAs (66); and (iv) the A loop at the end of helix 92 (though the lack of

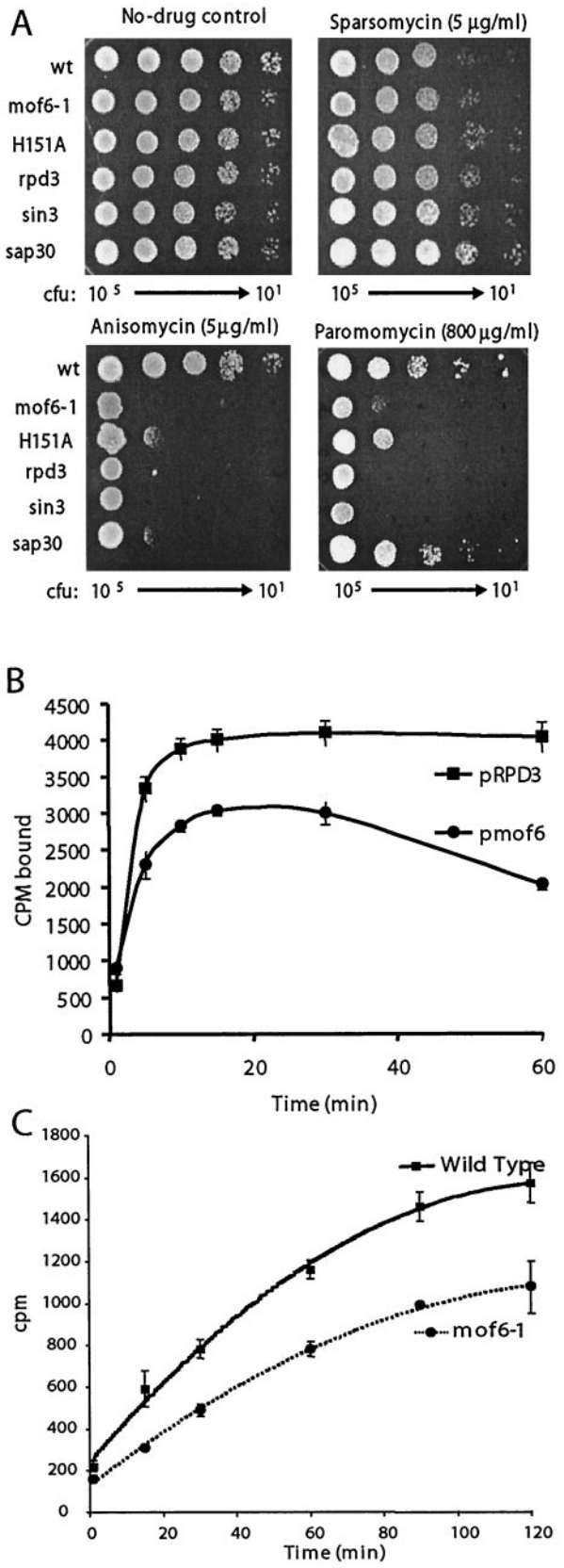

FIG. 6. The mutants promote ribosomal A site-specific and peptidyl transfer defects. (A) Pharmacogenetic analyses show hypersensitivity to A site-specific drugs. Tenfold dilutions (from 10^5 to 10^1 CFU) of isogenic wild-type, *rpd3*Δ, *mof6-1*, *rpd3-H151A*, *sin3*Δ, and *sap30*Δ strains were spotted onto selective (H−Trp) medium containing the indicated concentrations of drugs or no-drug controls and incubated at 30°C for 3 days. (B) Ribosomes from *mof6-1* cells have decreased binding for aa-tRNA. Ribosomes purified from isogenic wild-type and *mof6-1* strains were incubated with molar excess amounts of purified [^{14}C]Phe-tRNA, and salt-washed ribosomes were diluted at the indicated time points and quickly filtered through nitrocellulose filters. After drying, the filters were counted by liquid scintillation. Assays were performed in triplicate. Data points and error bars indicate means and standard deviations. (C) Ribosomes from *mof6-1* cells have decreased peptidyltransferase activities. Time course of the formation of [^{14}C]phenylalanine-puromycin product in assays using ribosomes isolated from isogenic *rpd3*Δ cells expressing wild-type or the *mof6-1* forms of Rpd3p. Ethyl acetate soluble radioactivity was determined by liquid scintillation counting. Control studies were performed in the absence of puromycin to determine the nonspecific extraction of CACCA[^{14}C]AcPhe. Control values (generally less than 2%) were subtracted from the values obtained in the presence of puromycin. All experiments were performed in triplicate. Data points and error bars indicate means and standard deviations.

effect of *mof6-1* ribosomes on acceptor fragment binding argues against the defect affecting this particular structure). Thus, an alternative to the altered heterochromatin topology hypothesis could be that a deficiency in the histone deacetylation machinery could result in repression of the RNA Pol II-transcribed box C+D and/or box H+ACA snoRNAs, which act as essential guides for base-specific rRNA modification (reviewed in references 13 and 53), resulting in the observed delay in 35S rRNA processing. Future studies will investigate this hypothesis directly, examining the base modification status of rRNAs in *mof6-1* mutants, the abundances of these snoRNAs, and the frameshifting and virus maintenance phenotypes of mutants defective in these processes.

Whatever its origin, the early delay in rRNA maturation affects a series of downstream processes involved in the biogenesis and functionality of ribosomes. These effects are specific to the formation and/or the function of the A site. The resulting ribosomes are less accurate than their wild-type counterparts and have decreased peptidyltransferase activities. The presence of these specific, rather than global, effects on ribosome function also provides strong arguments against the hypothesis that the observed frameshifting defects may be due to global misregulation of RP biosynthesis or to derepression of the *lacZ* frameshift reporter mRNAs. We hypothesize that the decreased rates of peptidyl transfer allow ribosomes with both A and P sites occupied by tRNAs to pause for longer periods of time at −1 frameshift signals, promoting increased −1 PRF efficiencies. Alternatively, decreased affinities of the mutant ribosomes for aa-tRNAs may make this tRNA more inclined to slip. Either of these mechanisms can account for the specific effect of *mof6-1* on programmed −1 ribosomal frameshifting and virus maintenance (20, 31).

Our observations also suggest that a functional histone deacetylase complex is essential for the proper timing and extent of downstream rRNA processing events and ribosome maturation. The delayed exit from lag-phase growth in the mutant cells suggests that limiting the availability of this complex is rate limiting with regard to these events. Corollary to this is that under such rate-limiting conditions, as the demand for new ribosomes outpaces the ability of the cell to supply

them, the cell would tend to produce a greater fraction of defective ribosomes in an attempt to keep up with demand. That the frameshifting defect is accentuated when the requirement for ribosomes is highest supports this bioeconomic hypothesis. Furthermore, the early entry of the mutants into diauxic shift shows that these cells are depleting the growth medium of carbon source at an accelerated rate. We hypothesize that functionally compromised ribosomes produce a large amount of inaccurately translated, inactive protein products. These dead-end protein products would be shunted to the protein degradation pathway, imposing a nonproductive energetic load on the mutant cells. By such a scenario, the bioenergetic cost per functional protein product would be substantially increased, which would account for the observation that these cells deplete the growth medium of carbon source and enter diauxic shift more rapidly than their wild-type counterparts.

ACKNOWLEDGMENTS

A.M. and J.L.B. contributed equally to this work.

We thank Andrew Vershon, Michael Hampsey, Lenore Neigeborn, and S. L. Shreiber for strains and clones and for helping to provide critical insights.

This work was supported by a grant to J.D.D. from the NIH (GM58859). J.L.B. was supported in part by a training grant from the NIH (T32 AI51967).

REFERENCES

1. **Abraham, A. K., and A. Pihl.** 1983. Effect of protein synthesis inhibitors on the fidelity of translation in eukaryotic systems. Biochim. Biophys. Acta **741:**197–203.
2. **Baim, S. B., D. F. Pietras, D. C. Eustice, and F. Sherman.** 1985. A mutation allowing an mRNA secondary structure diminishes translation of *Saccharomyces cerevisiae* iso-1-cytochrome *c*. Mol. Cell. Biol. **5:**1839–1846.
3. **Balasundaram, D., J. D. Dinman, C. W. Tabor, and H. Tabor.** 1994. Two essential genes in the biosynthesis of polyamines that modulate +1 ribosomal frameshifting in *Saccharomyces cerevisiae*. J. Bacteriol. **176:**7126–7128.
4. **Brierley, I.** 1995. Ribosomal frameshifting on viral RNAs. J. Gen. Virol. **76:**1885–1892.
5. **Bussey, H.** 1991. K1 killer toxin, a pore-forming protein from yeast. Mol. Microbiol. **5:**2339–2343.
6. **Carrasco, L., M. Barbacid, and D. Vazquez.** 1973. The tricodermin group of antibiotics, inhibitors of peptide bond formation by eukaryotic ribosomes. Biochim. Biophys. Acta **312:**368–376.
7. **Carr-Schmid, A., N. Durko, J. Cavallius, W. C. Merrick, and T. G. Kinzy.** 1999. Mutations in a GTP-binding motif of eukaryotic elongation factor 1A reduce both translational fidelity and the requirement for nucleotide exchange. J. Biol. Chem. **274:**30297–30302.
8. **Carter, A. P., W. M. Clemons, D. E. Brodersen, R. J. Morgan-Warren, B. T. Wimberly, and V. Ramakrishnan.** 2000. Functional insights from the structure of the 30S ribosomal subunit and its interactions with antibiotics. Nature **407:**340–348.
9. **Christianson, T. W., R. S. Sikorski, M. Dante, J. H. Shero, and P. Hieter.** 1992. Multifunctional yeast high-copy-number shuttle vectors. Yeast **110:** 119–122.
10. **Courey, A. J., and S. Jia.** 2001. Transcriptional repression: the long and the short of it. Genes Dev. **15:**2786–2796.
11. **Cui, Y., J. D. Dinman, T. G. Kinzy, and S. W. Peltz.** 1998. The Mof2/Sui1 protein is a general monitor of translational accuracy. Mol. Cell. Biol. **18:** 1506–1516.
12. **Cui, Y., J. D. Dinman, and S. W. Peltz.** 1996. *mof4-1* is an allele of the *UPF1/IFS2* gene which affects both mRNA turnover and −1 ribosomal frameshifting efficiency. EMBO J. **15:**5726–5736.
13. **Decatur, W. A., and M. J. Fournier.** 2002. rRNA modifications and ribosome function. Trends Biochem. Sci. **27:**344–351.
14. **Diedrich, G., C. M. Spahn, U. Stelzl, M. A. Schafer, T. Wooten, D. E. Bochkariov, B. S. Cooperman, R. R. Traut, and K. H. Nierhaus.** 2000. Ribosomal protein L2 is involved in the association of the ribosomal subunits, tRNA binding to A and P sites and peptidyl transfer. EMBO J. **19:**5241–5250.
15. **Dinman, J. D., T. Icho, and R. B. Wickner.** 1991. A −1 ribosomal frameshift in a double-stranded RNA virus forms a gag-pol fusion protein. Proc. Natl. Acad. Sci. USA **88:**174–178.
16. **Dinman, J. D., and T. G. Kinzy.** 1997. Translational misreading: mutations in translation elongation factor 1α differentially affect programmed ribosomal frameshifting and drug sensitivity. RNA **3:**870–881.
17. **Dinman, J. D., M. J. Ruiz-Echevarria, K. Czaplinski, and S. W. Peltz.** 1997. Peptidyl transferase inhibitors have antiviral properties by altering programmed −1 ribosomal frameshifting efficiencies: development of model systems. Proc. Natl. Acad. Sci. USA **94:**6606–6611.
18. **Dinman, J. D., M. J. Ruiz-Echevarria, and S. W. Peltz.** 1998. Translating old drugs into new treatments: identifying compounds that modulate programmed −1 ribosomal frameshifting and function as potential antiviral agents. Trends Biotechnol. **16:**190–196.
19. **Dinman, J. D., and R. B. Wickner.** 1992. Ribosomal frameshifting efficiency and *gag/gag-pol* ratio are critical for yeast M_1 double-stranded RNA virus propagation. J. Virol. **66:**3669–3676.
20. **Dinman, J. D., and R. B. Wickner.** 1994. Translational maintenance of frame: mutants of *Saccharomyces cerevisiae* with altered −1 ribosomal frameshifting efficiencies. Genetics **136:**75–86.
21. **Dinman, J. D., and R. B. Wickner.** 1995. 5S rRNA is involved in fidelity of translational reading frame. Genetics **141:**95–105.
22. **Dragon, F., J. E. Gallagher, P. A. Compagnone-Post, B. M. Mitchell, K. A. Porwancher, K. A. Wehner, S. Wormsley, R. E. Settlage, J. Shabanowitz, Y. Osheim, A. L. Beyer, D. F. Hunt, and S. J. Baserga.** 2002. A large nucleolar U3 ribonucleoprotein required for 18S ribosomal RNA biogenesis. Nature **417:**967–970.
23. **Dunbar, D. A., S. Wormsley, T. M. Agentis, and S. J. Baserga.** 1997. Mpp10p, a U3 small nucleolar ribonucleoprotein component required for pre-18S rRNA processing in yeast. Mol. Cell. Biol. **17:**5803–5812.
24. **Farabaugh, P. J.** 1996. Programmed translational frameshifting. Microbiol. Rev. **60:**103–134.
25. **Fath, S., P. Milkereit, A. V. Podtelejnikov, N. Bischler, P. Schultz, M. Bier, M. Mann, and H. Tschochner.** 2000. Association of yeast RNA polymerase I with a nucleolar substructure active in rRNA synthesis and processing. J. Cell Biol. **149:**575–589.
26. **Fried, H. M., and G. R. Fink.** 1978. Electron microscopic heteroduplex analysis of "killer" double-stranded RNA species from yeast. Proc. Natl. Acad. Sci. USA **75:**4224–4228.
27. **Fujimura, T., and R. B. Wickner.** 1992. Interaction of two *cis* sites with the RNA replicase of the yeast L-A virus. J. Biol. Chem. **267:**2708–2713.
28. **Gesteland, R. F., and J. F. Atkins.** 1996. Recoding: dynamic reprogramming of translation. Annu. Rev. Biochem. **65:**741–768.
29. **Grollman, A. P.** 1967. Inhibitors of protein biosynthesis. II. Mode of action of anisomycin. J. Biol. Chem. **242:**3226–3233.
30. **Haenni, A. L., and F. Chapeville.** 1966. The behaviour of acetylphenylalanyl soluble ribonucleic acid in polyphenylalanine synthesis. Biochim. Biophys. Acta **114:**135–148.
31. **Harger, J. W., A. Meskauskas, and J. D. Dinman.** 2002. An "integrated model" of programmed ribosomal frameshifting and post-transcriptional surveillance. Trends Biochem. Sci. **27:**448–454.
32. **Harris, R., and S. Pestka.** 1973. Studies on the formation of transfer ribonucleic acid-ribosome complexes. XXIV. Effects of antibiotics on binding of aminoacyl-oligonucleotides to ribosomes. J. Biol. Chem. **248:**1168–1174.
33. **Hassig, C. A., T. C. Fleischer, A. N. Billin, S. L. Schreiber, and D. E. Ayer.** 1997. Histone deacetylase activity is required for full transcriptional repression by mSin3A. Cell **89:**341–347.
34. **Herner, A. E., I. H. Goldberg, and L. B. Cohen.** 1969. Stabilization of *N*-acetylphenylalanyl transfer ribonucleic acid binding to ribosomes by sparsomycin. Biochemistry **8:**1335–1344.
35. **Icho, T., and R. B. Wickner.** 1989. The double-stranded RNA genome of yeast virus L-A encodes its own putative RNA polymerase by fusing two open reading frames. J. Biol. Chem. **264:**6716–6723.
36. **Ito, H., Y. Fukuda, K. Murata, and A. Kimura.** 1983. Transformation of intact yeast cells treated with alkali cations. J. Bacteriol. **153:**163–168.
37. **Jacks, T., H. D. Madhani, F. R. Masiraz, and H. E. Varmus.** 1988. Signals for ribosomal frameshifting in the Rous sarcoma virus *gag-pol* region. Cell **55:** 447–458.
38. **Jacks, T., and H. E. Varmus.** 1985. Expression of the Rous sarcoma virus pol gene by ribosomal frameshifting. Science **230:**1237–1242.
39. **Jayaraman, J., and I. H. Goldberg.** 1968. Localization of sparsomycin action to the peptide-bond-forming step. Biochemistry **7:**418–421.
40. **Kadosh, D., and K. Struhl.** 1998. Histone deacetylase activity of Rpd3 is important for transcriptional repression in vivo. Genes Dev. **12:**797–805.
41. **Kasten, M. M., S. Dorland, and D. J. Stillman.** 1997. A large protein complex containing the yeast Sin3p and Rpd3p transcriptional regulators. Mol. Cell. Biol. **17:**4852–4858.
42. **Kressler, D., P. Linder, and C. J. de La Cruz.** 1999. Protein *trans*-acting factors involved in ribosome biogenesis in *Saccharomyces cerevisiae*. Mol. Cell. Biol. **19:**7897–7912.
43. **Kunkel, T.** 1985. Rapid and efficient site-specific mutagenesis without phenotype selection. Proc. Natl. Acad. Sci. USA **82:**488–492.
44. **Leary, D. J., and S. Huang.** 2001. Regulation of ribosome biogenesis within the nucleolus. FEBS Lett. **509:**145–150.
45. **Lee, S. J., and S. J. Baserga.** 1999. Imp3p and Imp4p, two specific compo-

nents of the U3 small nucleolar ribonucleoprotein that are essential for pre-18S rRNA processing. Mol. Cell. Biol. **19:**5441–5452.
46. **Liermann, R. T., J. D. Dinman, L. A. Sylvers, and J. C. Jackson.** 2000. Improved purification of the double-stranded RNA from killer strains of yeast. BioTechniques **28:**64–65.
47. **Lopinski, J. D., J. D. Dinman, and J. A. Bruenn.** 2000. Kinetics of ribosomal pausing during programmed −1 translational frameshifting. Mol. Cell. Biol. **20:**1095–1103.
48. **Merrick, W. C.** 1979. Assays for eukaryotic protein synthesis. Methods Enzymol. **60:**108–123.
49. **Meskauskas, A., and J. D. Dinman.** Decreased peptidyltransferase activity correlates with increased programmed −1 ribosomal frameshifting and viral maintenance defects in the yeast *Saccharomyces cerevisiae*. RNA, in press.
50. **Meskauskas, A., and J. D. Dinman.** 2001. Ribosomal protein L5 helps anchor peptidyl-tRNA to the P-site in *Saccharomyces cerevisiae*. RNA **7:**1084–1096.
51. **Moazed, D., and H. F. Noller.** 1991. Sites of interaction of the CCA end of peptidyl-tRNA with 23S rRNA. Proc. Natl. Acad. Sci. USA **88:**3725–3728.
52. **Nissen, P., J. A. Ippolito, N. Ban, P. B. Moore, and T. A. Steitz.** 2001. RNA tertiary interactions in the large ribosomal subunit: the A-minor motif. Proc. Natl. Acad. Sci. USA **98:**4899–4903.
53. **Ofengand, J.** 2002. Ribosomal RNA pseudouridines and pseudouridine synthases. FEBS Lett. **514:**17–25.
54. **Ogle, J. M., D. E. Brodersen, W. M. Clemons, Jr., M. J. Tarry, A. P. Carter, and V. Ramakrishnan.** 2001. Recognition of cognate transfer RNA by the 30S ribosomal subunit. Science **292:**897–902.
55. **Ohtake, Y., and R. B. Wickner.** 1995. Yeast virus propagation depends critically on free 60S ribosomal subunit concentration. Mol. Cell. Biol. **15:**2772–2781.
56. **Peltz, S. W., A. B. Hammell, Y. Cui, J. Yasenchak, L. Puljanowski, and J. D. Dinman.** 1999. Ribosomal protein L3 mutants alter translational fidelity and promote rapid loss of the yeast killer virus. Mol. Cell. Biol. **19:**384–391.
57. **Pestka, S., T. Hishizawa, and J. L. Lessard.** 1970. Studies on the formation of transfer ribonucleic acid-ribosome complexes. 8. Aminoacyl oligonucleotide binding to ribosomes: characteristics and requirements. J. Biol. Chem. **245:**6208–6219.
58. **Rose, M. D., P. Novick, J. H. Thomas, D. Botstein, and G. R. Fink.** 1987. A *Saccharomyces cerevisiae* genomic plasmid bank based on a centromere-containing shuttle vector. Gene **60:**237–243.
59. **Ruiz-Echevarria, M. J., J. M. Yasenchak, X. Han, J. D. Dinman, and S. W. Peltz.** 1998. The Upf3p protein is a component of the surveillance complex that monitors both translation and mRNA turnover and affects viral maintenance. Proc. Natl. Acad. Sci. USA **95:**8721–8726.
60. **Sambrook, J., E. F. Fritsch, and T. Maniatis.** 1989. Molecular cloning: a laboratory manual, 2nd ed. Cold Spring Harbor Laboratory Press, Cold Spring Harbor, N.Y.
61. **Schena, M., and K. Yamamoto.** 1988. Mammalian glucocorticoid receptor derivatives enhance transcription in yeast. Science **241:**965–967.
62. **Schindler, D.** 1974. Two classes of inhibitors of peptidyl transferase activity in eukaryotes. Nature **249:**38–41.
63. **Sikorski, R. S., and P. Hieter.** 1989. A system of shuttle vectors and yeast host strains designed for efficient manipulation of DNA in *Saccharomyces cerevisiae*. Genetics **122:**19–27.
64. **Smith, M. W., A. Meskauskas, P. Wang, P. V. Sergiev, and J. D. Dinman.** 2001. Saturation mutagenesis of 5S rRNA in *Saccharomyces cerevisiae*. Mol. Cell. Biol. **21:**8264–8275.
65. **Somogyi, P., A. J. Jenner, I. A. Brierley, and S. C. Inglis.** 1993. Ribosomal pausing during translation of an RNA pseudoknot. Mol. Cell. Biol. **13:**6931–6940.
66. **Stark, H., M. V. Rodnina, H. J. Wieden, F. Zemlin, W. Wintermeyer, and M. van Heel.** 2002. Ribosome interactions of aminoacyl-tRNA and elongation factor Tu in the codon-recognition complex. Nat. Struct. Biol. **9:**849–854.
67. **Struhl, K.** 1998. Histone acetylation and transcriptional regulatory mechanisms. Genes Dev. **12:**599–606.
68. **Suka, N., A. A. Carmen, S. E. Rundlett, and M. Grunstein.** 1998. The regulation of gene activity by histones and the histone deacetylase RPD3. Cold Spring Harbor Symp. Quant. Biol. **63:**391–399.
69. **Sun, Z. W., and M. Hampsey.** 1999. A general requirement for the Sin3-Rpd3 histone deacetylase complex in regulating silencing in *Saccharomyces cerevisiae*. Genetics **152:**921–932.
70. **Taunton, J., C. A. Hassig, and S. L. Schreiber.** 1996. A mammalian histone deacetylase related to the yeast transcriptional regulator Rpd3p. Science **272:**408–411.
71. **Thompson, J. D., D. G. Higgins, and T. J. Gibson.** 1994. CLUSTAL W: improving the sensitivity of progressive multiple sequence alignment through sequence weighting, position-specific gap penalties and weight matrix choice. Nucleic Acids Res. **22:**4673–4680.
72. **Tu, C., T.-H. Tzeng, and J. A. Bruenn.** 1992. Ribosomal movement impeded at a pseudoknot required for ribosomal frameshifting. Proc. Natl. Acad. Sci. USA **89:**8636–8640.
73. **Tumer, N. E., B. Parikh, P. Li, and J. D. Dinman.** 1998. Pokeweed antiviral protein specifically inhibits Ty*1* directed +1 ribosomal frameshifting and Ty*1* retrotransposition in *Saccharomyces cerevisiae*. J. Virol. **72:**1036–1042.
74. **Tzeng, T.-H., C. L. Tu, and J. A. Bruenn.** 1992. Ribosomal frameshifting requires a pseudoknot in the *Saccharomyces cerevisiae* double-stranded RNA virus. J. Virol. **66:**999–1006.
75. **Venema, J., and D. Tollervey.** 1999. Ribosome synthesis in *Saccharomyces cerevisiae*. Annu. Rev. Genet. **33:**261–311.
76. **Vershon, A. K., N. M. Hollingsworth, and A. D. Johnson.** 1992. Meiotic induction of the yeast HOP1 gene is controlled by positive and negative regulatory sites. Mol. Cell. Biol. **12:**3706–3714.
77. **Vicens, Q., and E. Westhof.** 2001. Crystal structure of paromomycin docked into the eubacterial ribosomal decoding A site. Structure **9:**647–658.
78. **Vidal, M., and R. F. Gaber.** 1991. RPD3 encodes a second factor required to achieve maximum positive and negative transcriptional states in *Saccharomyces cerevisiae*. Mol. Cell. Biol. **11:**6317–6327.
79. **Wang, A. H., N. R. Bertos, M. Vezmar, N. Pelletier, M. Crosato, H. H. Heng, J. Th'ng, J. Han, and X. J. Yang.** 1999. HDAC4, a human histone deacetylase related to yeast HDA1, is a transcriptional corepressor. Mol. Cell. Biol. **19:**7816–7827.
80. **Warner, J. R.** 1999. The economics of ribosome biosynthesis in yeast. Trends Biochem. Sci. **24:**437–440.
81. **Wickner, R. B.** 1996. Double-stranded RNA viruses of *Saccharomyces cerevisiae*. Microbiol. Rev. **60:**250–265.
82. **Wickner, R. B., and M. J. Leibowitz.** 1976. Two chromosomal genes required for killing expression in killer strains of *Saccharomyces cerevisiae*. Genetics **82:**429–442.